CEITEC

Central European Institute of Technology

BRNO | CZECH REPUBLIC

Journal club: Adineh et al., 2016

C9940 3-Dimensional Transmission Electron Microscopy
S1007 Doing structural biology with the electron microscope

May 29, 2017

EUROPEAN UNION
EUROPEAN REGIONAL DEVELOPMENT FUND
INVESTING IN YOUR FUTURE

2007–13
OP Research and
Development for Innovation

FIRST:
Fourier Shell Correlation, revisited

Fourier Shell Correlation (FSC)

Reconstruction 1

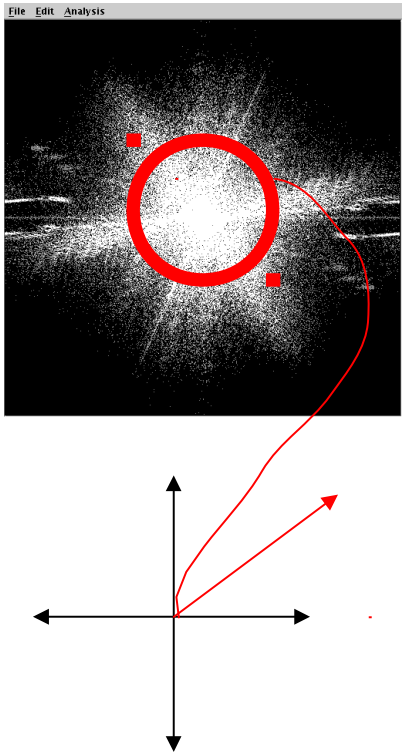

term A1

Reconstruction 2

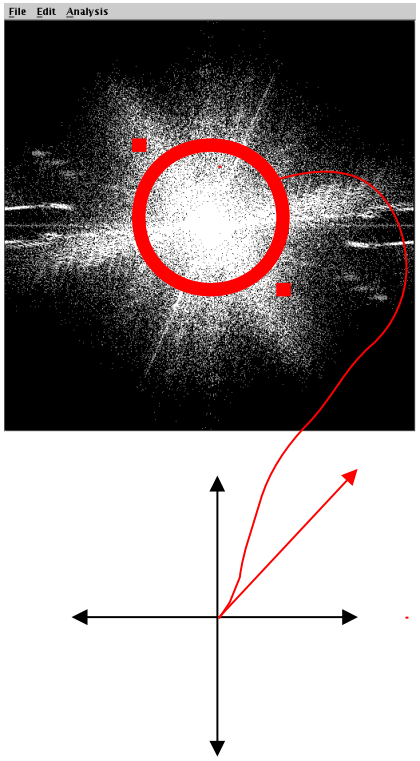

term 2

Properties:
- Fourier terms have amplitude + phase.
- Correlation values range from -1 to +1.
- Noise should give an average of 0.
- The comparison is done as a function of spatial frequency (or “resolution”)

Fourier Shell Correlation (FSC)

Reconstruction 1

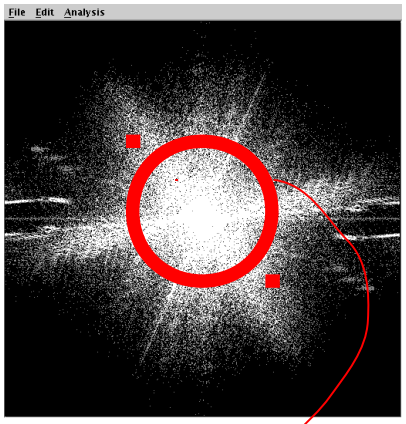

Reconstruction 2

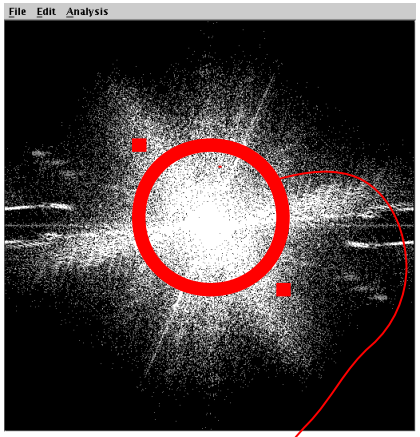

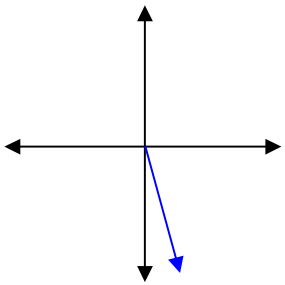

term B1

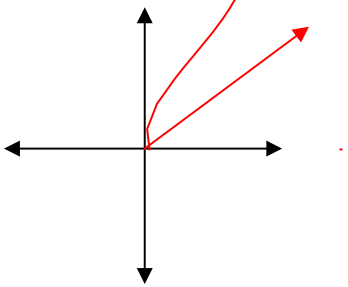

term A1

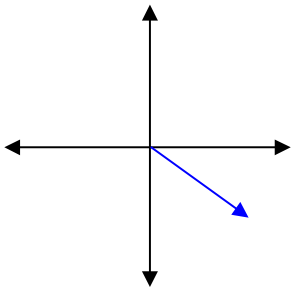

term B2

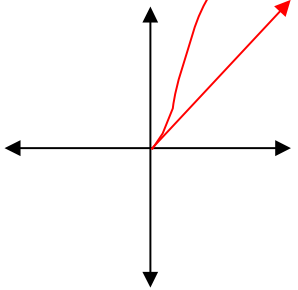

term A2

$$FSC(r) = \frac{\sum_{r_i \in r} F_1(r_i) \cdot F_2(r_i)^*}{\sqrt{\sum_{r_i \in r} |F_1(r_i)|^2 \cdot \sum_{r_i \in r} |F_2(r_i)|^2}}$$

Fourier Shell Correlation (FSC)

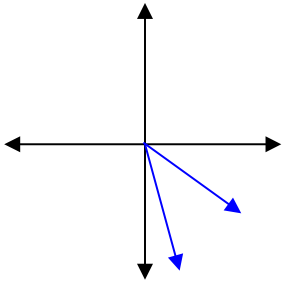

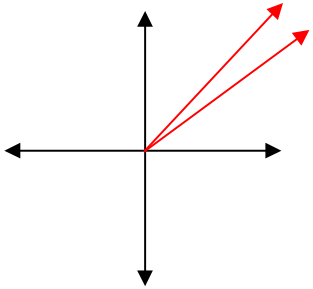

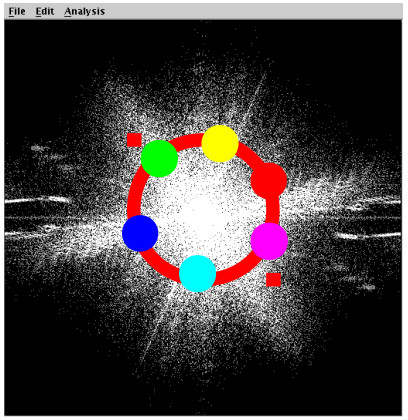

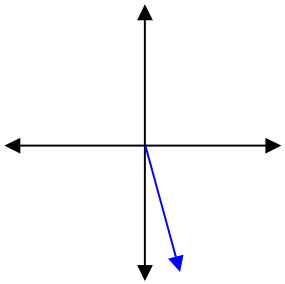

term B1

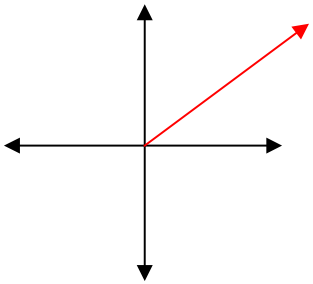

term A1

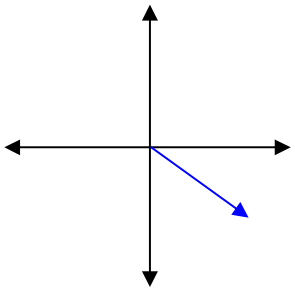

term B2

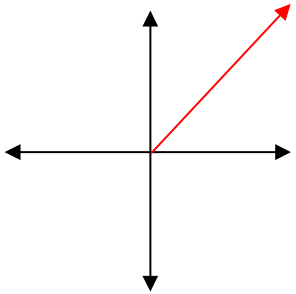

term A2

$$FSC(r) = \frac{\sum_{r_i \in r} F_1(r_i) \cdot F_2(r_i)^*}{\sqrt[2]{\sum_{r_i \in r} |F_1(r_i)|^2 \cdot \sum_{r_i \in r} |F_2(r_i)|^2}}$$

Fourier Shell Correlation (FSC)

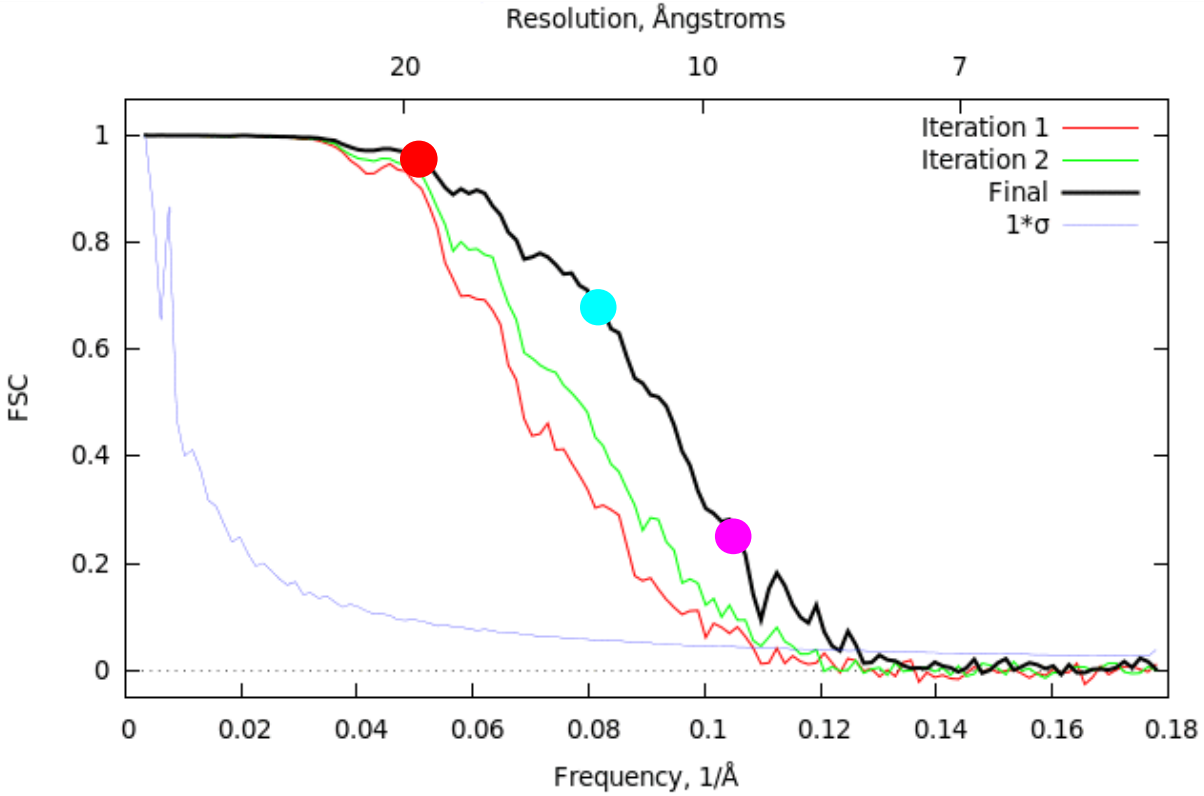

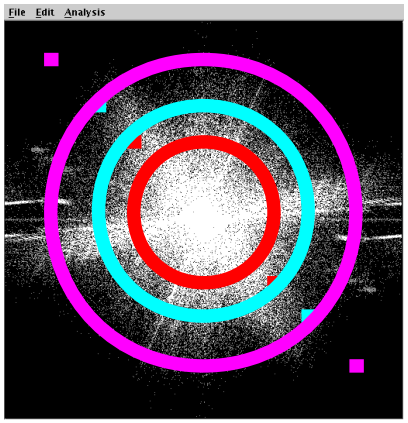

Adineh et al., 2016

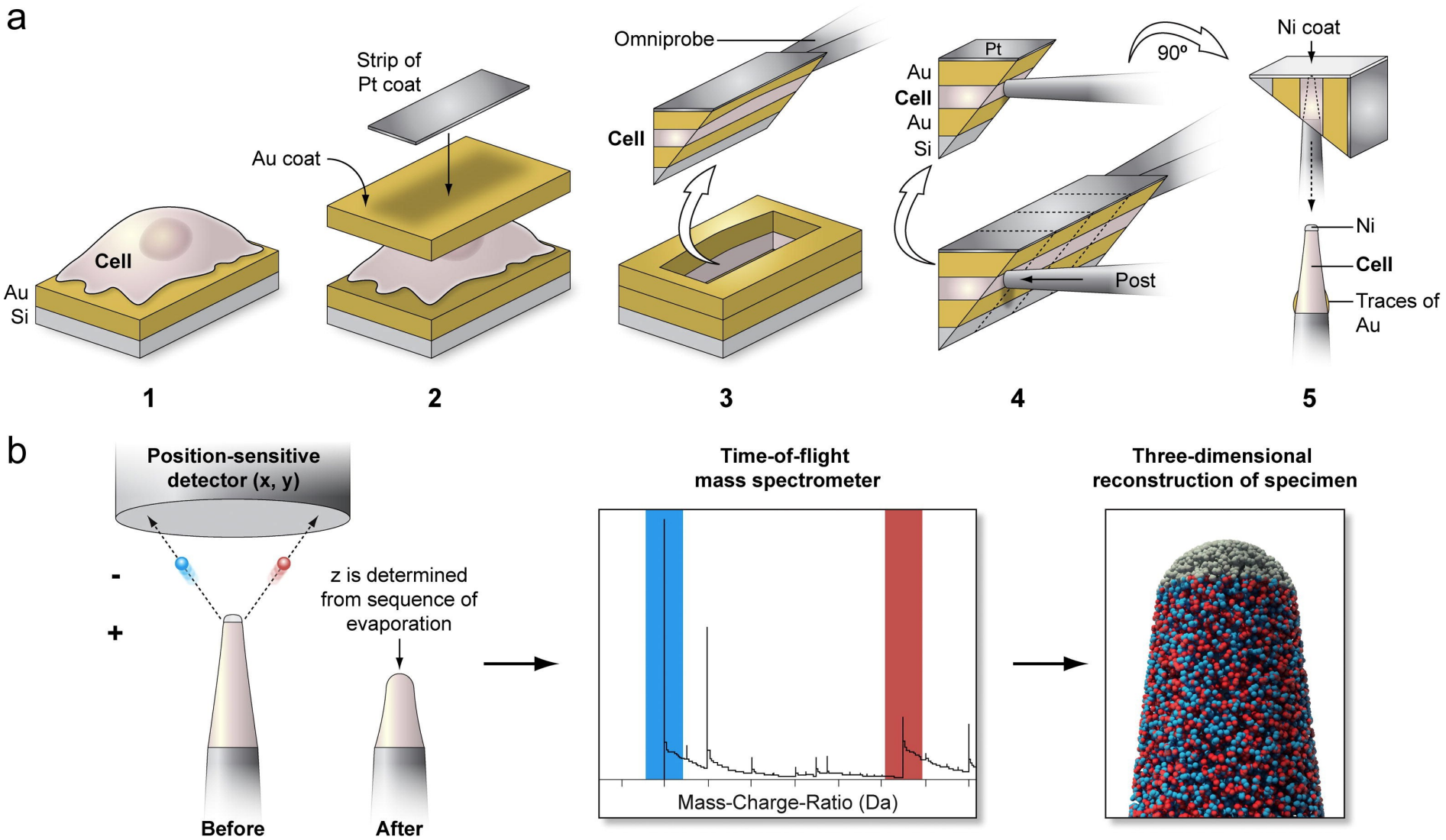

Schematic for the cellular sample preparation and APT data acquisition run (a) HeLa cells grown on gold-coated silicon substrates were coated with a thick layer of gold followed by a strip of platinum for further protection. Using FIB based protocols, a wedge containing a “sandwiched” cell volume was extracted and a sub-volume was attached to a microtip post in an orthogonal orientation. Following another protective nickel coat, the sub-volume was shaped into an APT-amenable tip by further FIB milling. (b) During an APT acquisition run, ions from the tip are extracted and are detected by a position-sensitive detector; this part of the tip is consumed as a result. Time-of-flight measurements of these detected ions allows their chemical identification in a mass spectrum, and a reverse-point algorithm can then be used to spatially place the ions in a high resolution reconstruction of the original tip.

Narayan... Subramaniam, 2012, J. Struct. Biol

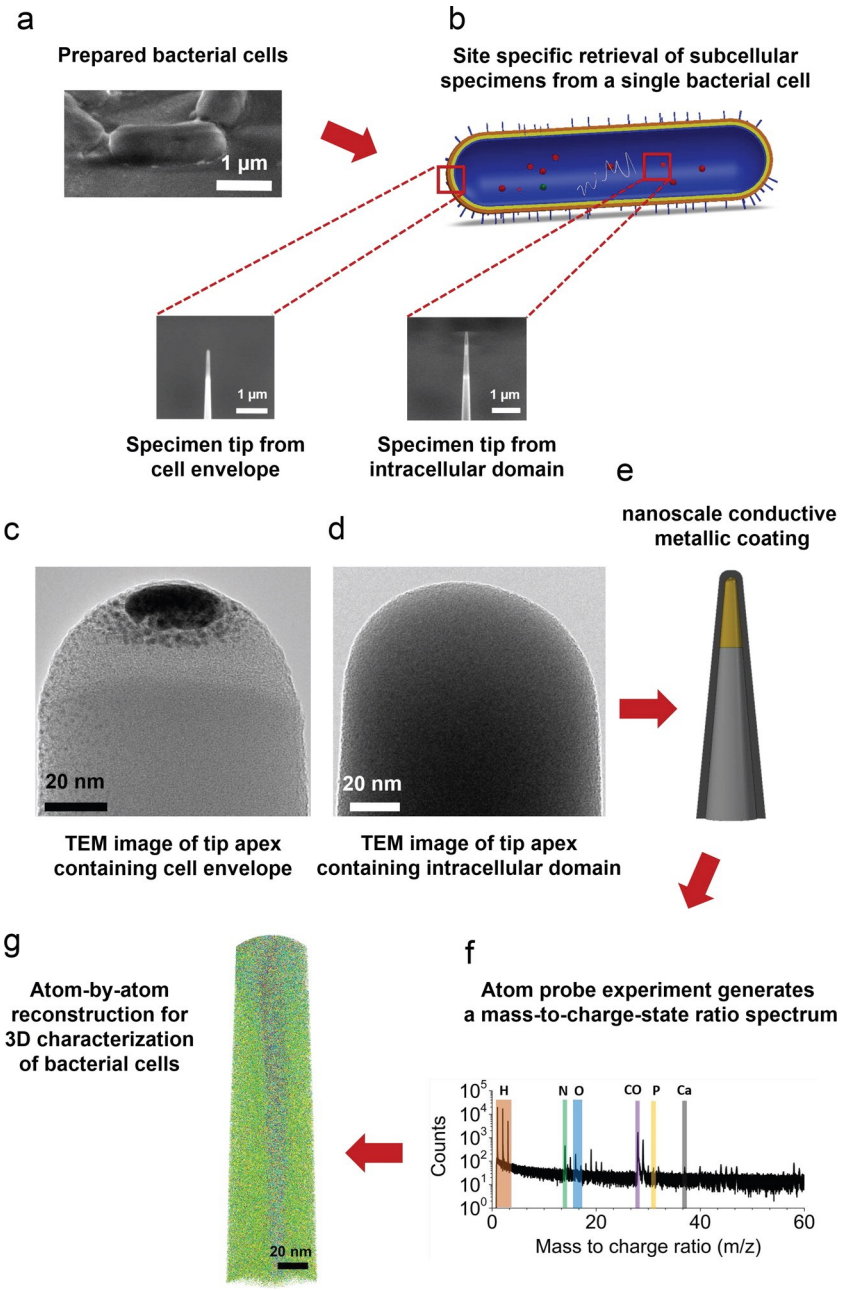

Figure 1. Schematic of the proposed approach for site-specific 3D atomic-scale analysis of bacterial cells. (a) A specimen from a single bacterial cells was retrieved using FIB-lift-out technique, and (b) a site-specific final needle-shaped specimen tip was achieved by precise annular FIB milling and contained a specific region of the original cell (either cell envelope or intracellular domain). (c−d) Selected site specific needle-shaped specimens from the cell envelope and intracellular domains were observed with conventional TEM. (e) Prior to APT, sufficient electrical conductivity is achieved with a nanoscale layer of metallic coating, which allows field evaporation of the specimen tip via pulsed-voltage APT and leads to (f) a mass-to-charge-state ratio spectrum of the ionic species followed by (g) an actual 3D reconstruction of the tomographic map at near-atomic resolution.

CEITEC

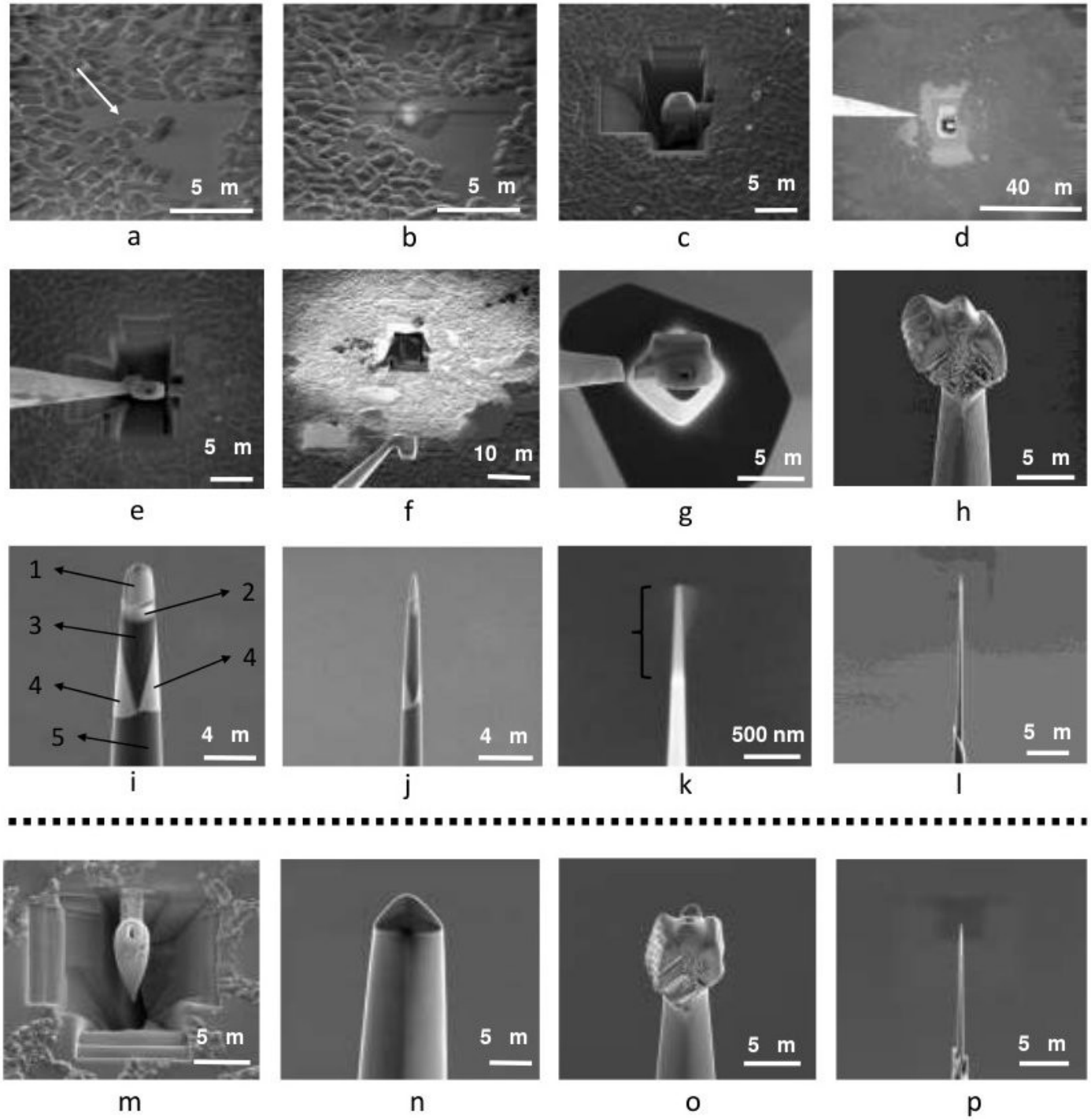

Supporting Figure 1: SEM images taken during the FIB lift-out process to create APT specimen from bacterial cells.

CEITEC

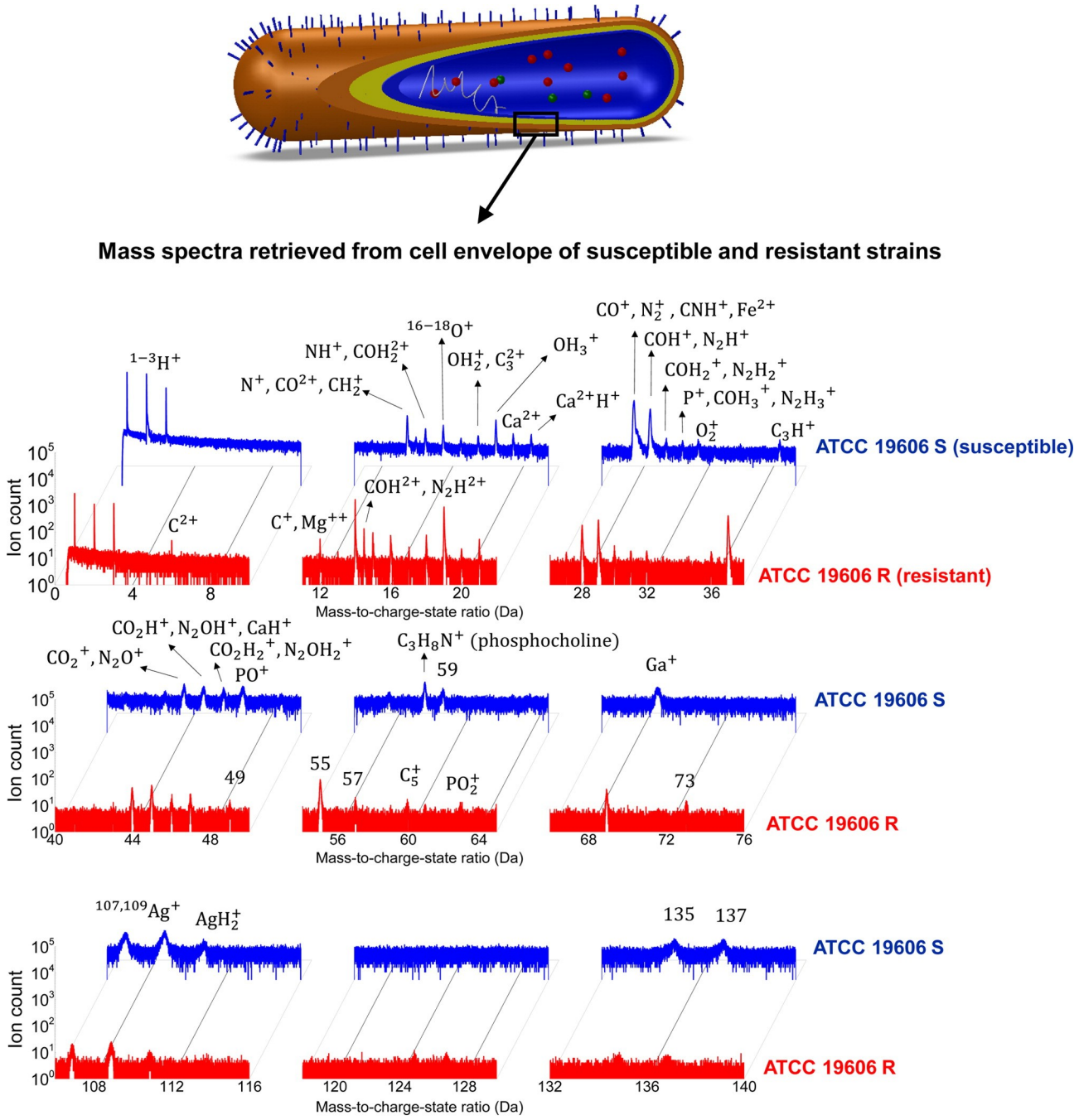

Figure 2. Mass-to-charge-state ratio spectra acquired from the cell envelope of *A. baumannii*, revealing distinct information from both a susceptible strain (ATCC 19606 S) highlighted in blue and a resistant strain (ATCC 19606 R) highlighted in red.

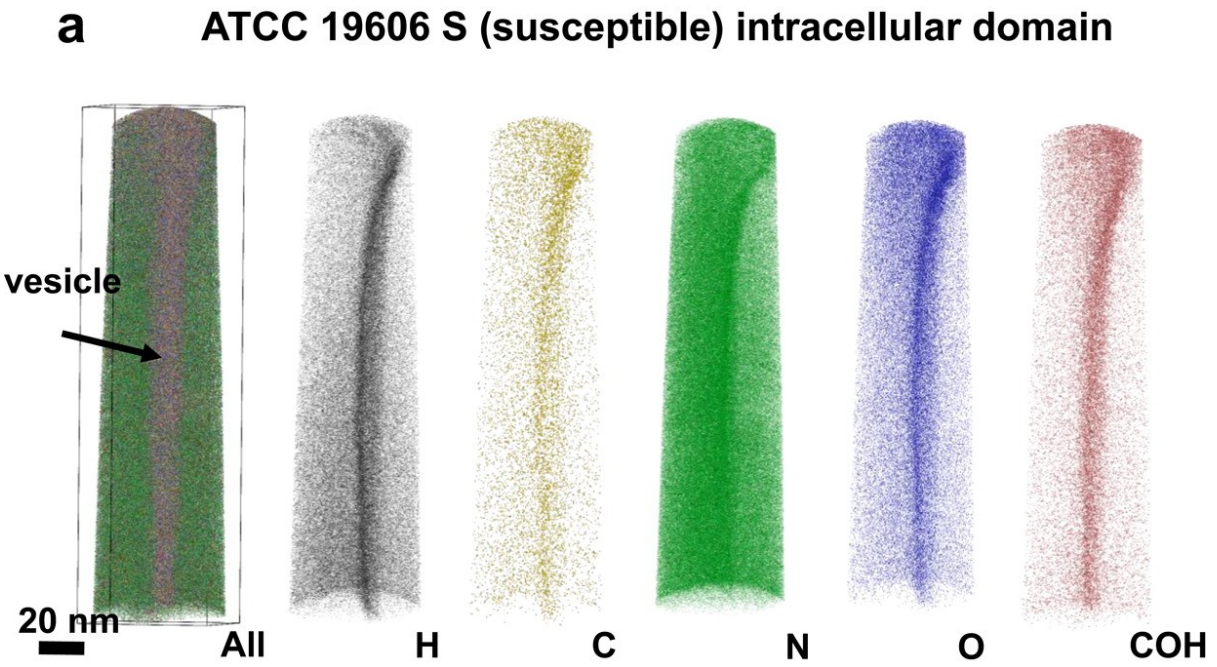

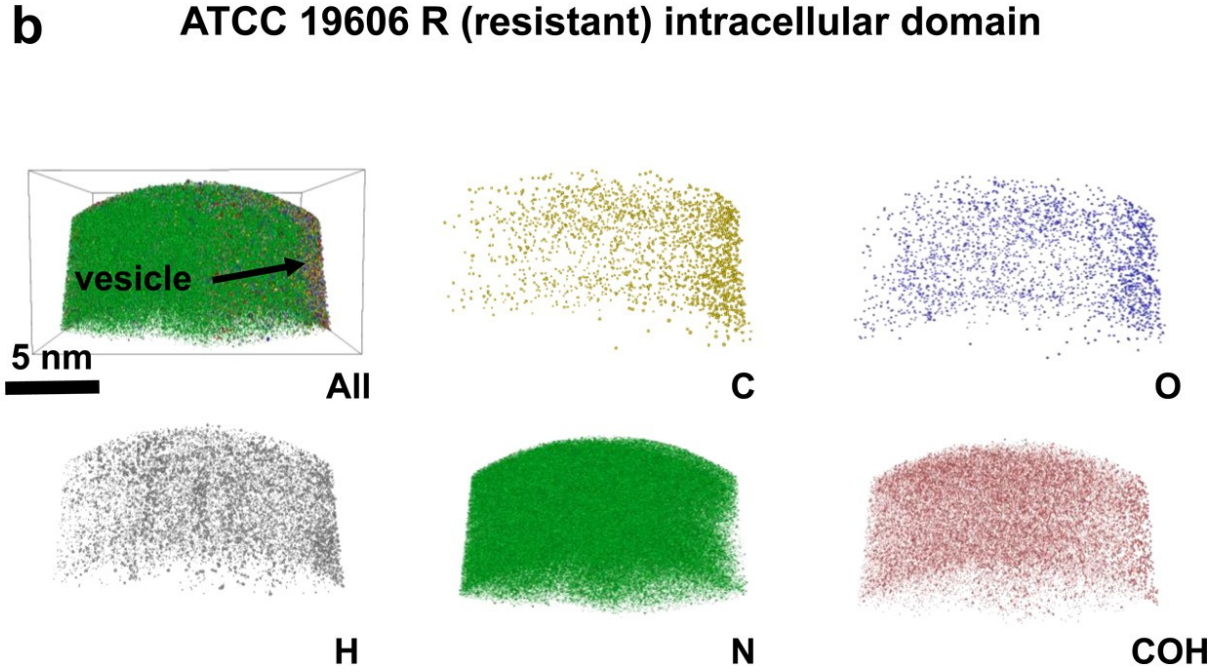

Figure 3. 3D ion species maps from the APT reconstructions of (a) intracellular domain of a susceptible strain and (b) intracellular domain of a resistant strain.

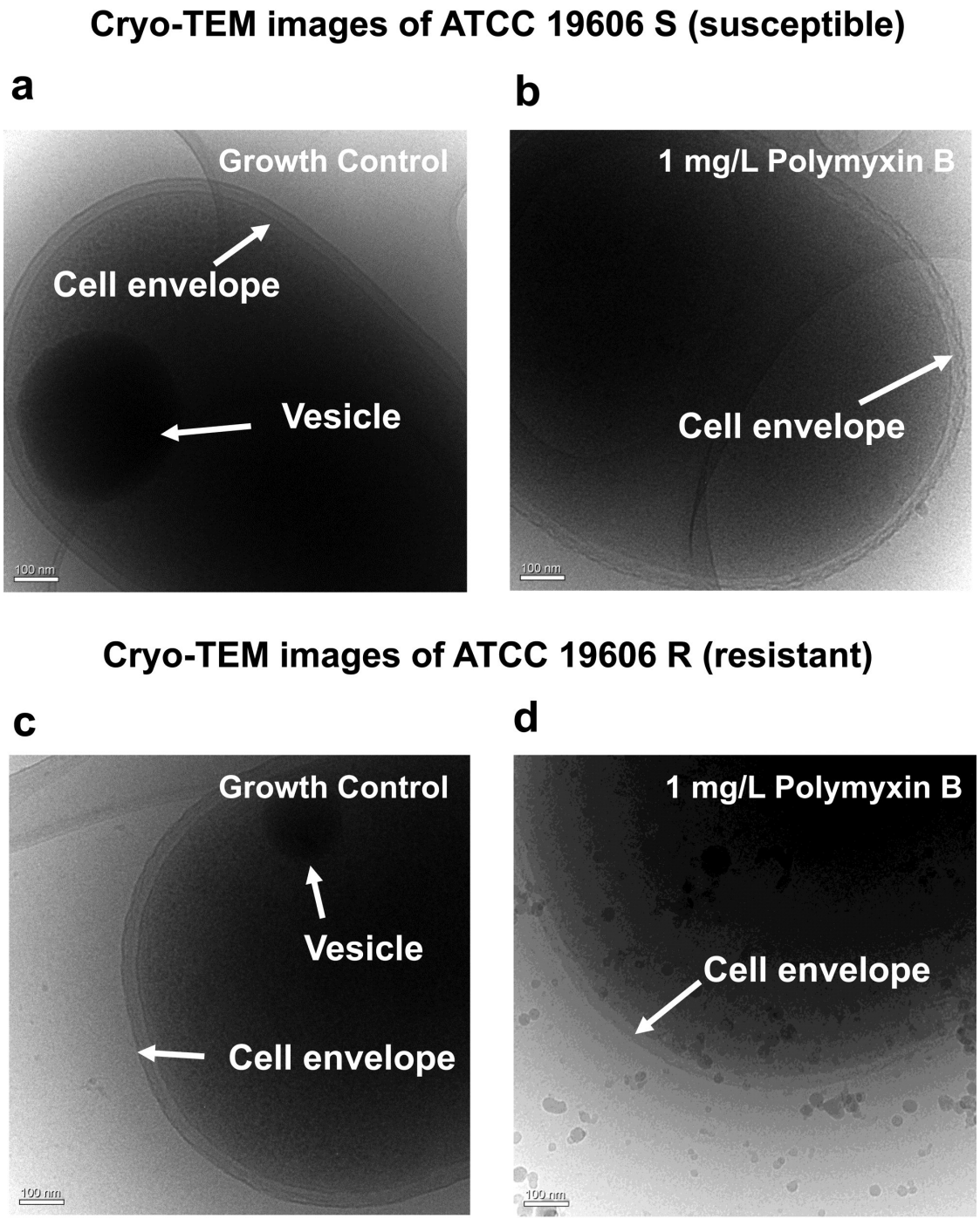

Figure 4. Cryo-TEM images of the cell envelope from (a) control and (b) polymyxin B treated A. baumannii susceptible strain (ATCC19606 S) and from the control and polymyxin B treated resistant strain (ATCC19606 R) in (c) and (d), respectively.

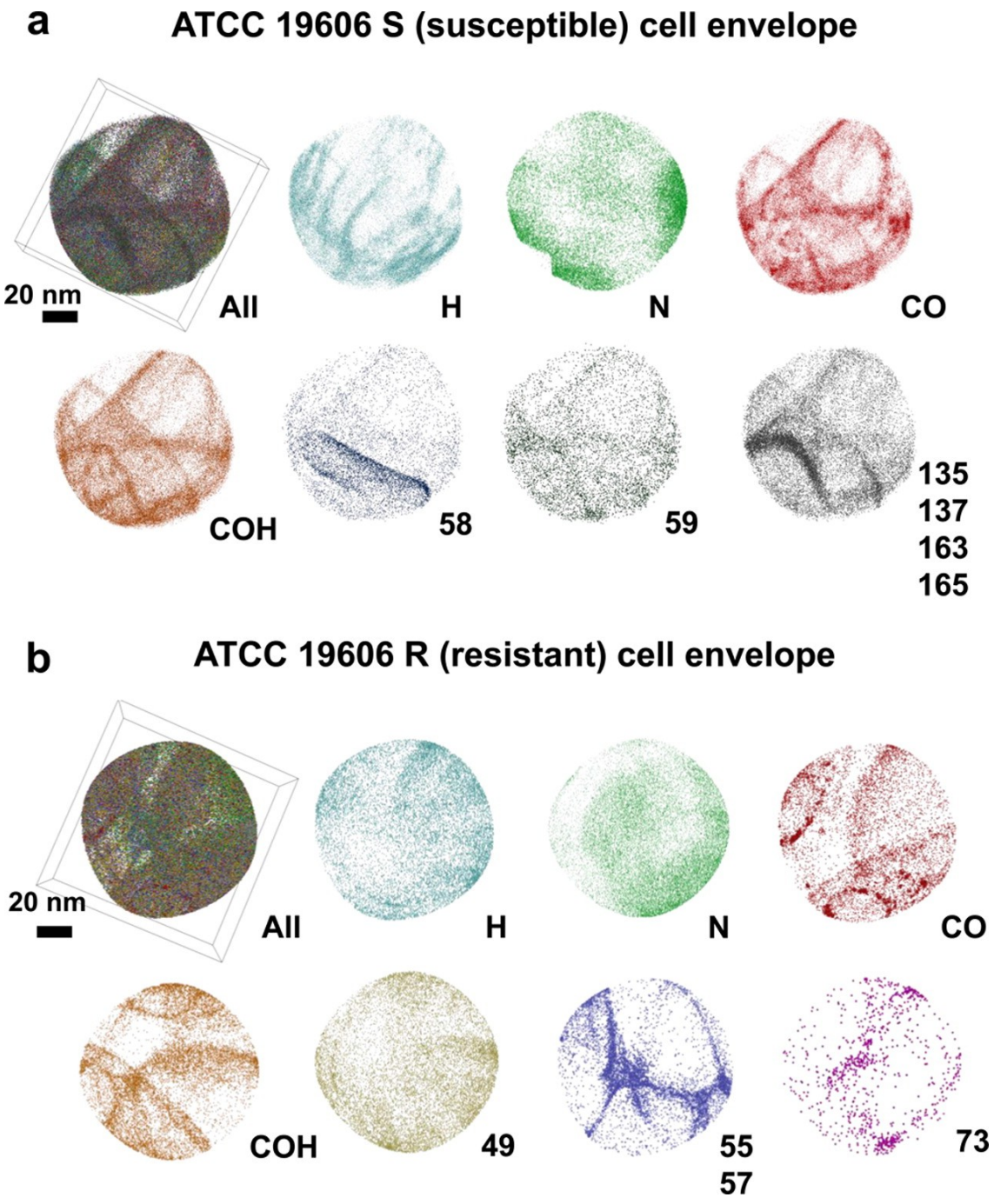

Figure 5. 3D ion species maps from the APT reconstructions of (a) cell envelope of susceptible strain, and (b) cell envelope of resistant strain.

DISCUSSION

Thank you for your attention

CEITEC

Central European Institute of Technology
Masaryk University
Kamenice 753/5
625 00 Brno, Czech Republic

www.ceitec.muni.cz | info@ceitec.muni.cz

UNIVERSITAS MASARYKIANA BRUNENSIS

EUROPEAN UNION
EUROPEAN REGIONAL DEVELOPMENT FUND
INVESTING IN YOUR FUTURE

2007–13
OP Research and Development for Innovation

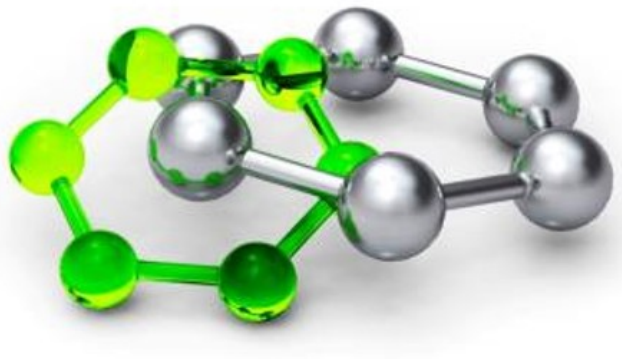

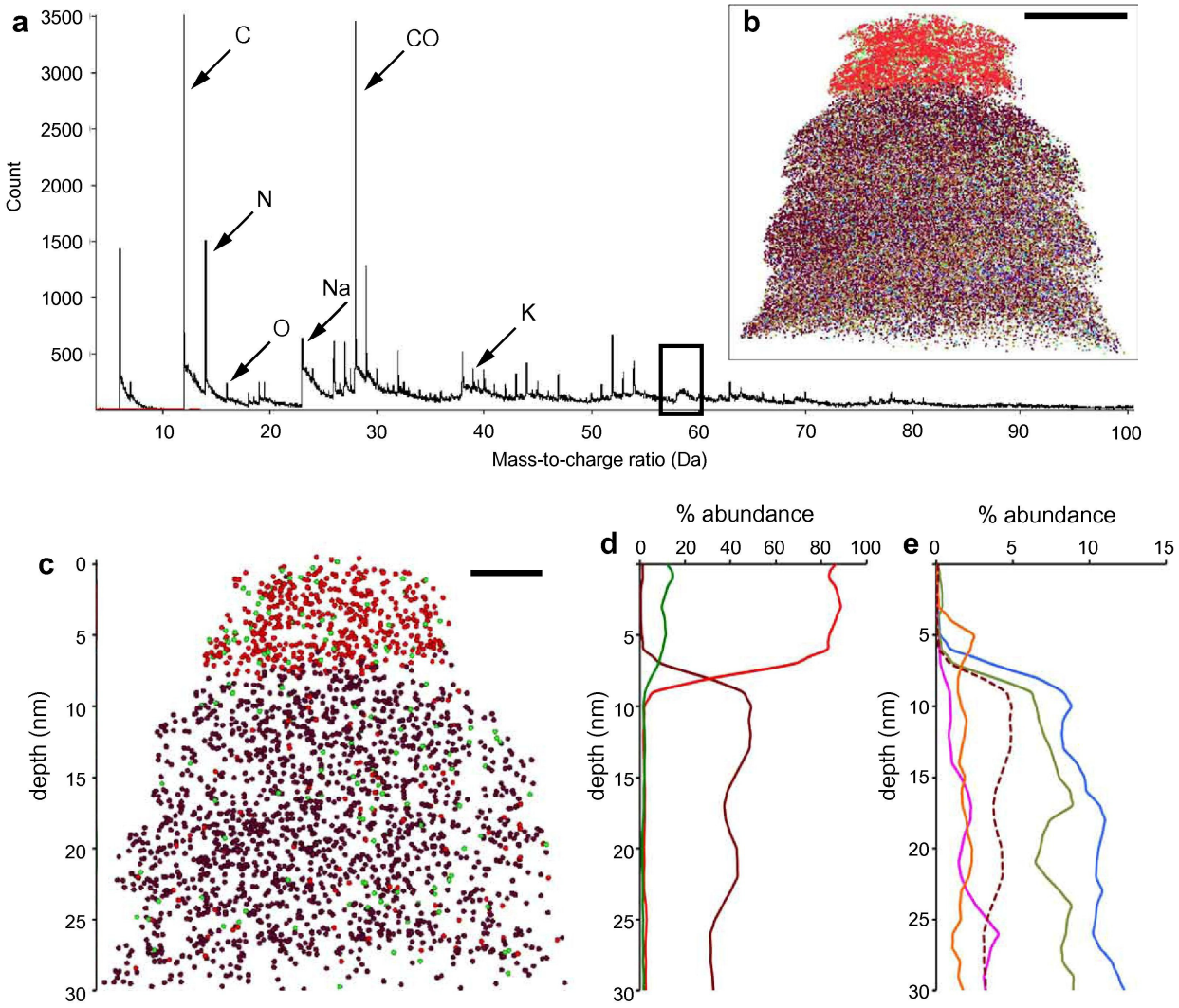

Narayan... Subramaniam, 2012, J. Struct. Biol

Cellular tips can be accurately reconstructed
(a) Mass spectrum of first 1.5 × 10 6 ions field evaporated from the tip, plotted in 0.01 Da bins. The broad peak corresponding to nickel is boxed, and relevant ions plotted in the reconstruction are marked. (b) Corresponding 3D reconstruction of this part of the tip. (c) 10 nm slice from the central plane of the reconstruction, showing distribution of selected ions nickel (red), gallium (green) and carbon (brown). (d) Corresponding plot of % abundance of these ions versus depth along the z axis. (e) Plot of % abundance versus depth of less abundant ions, nitrogen (blue), potassium (green), oxygen (orange) and sodium (pink) of the
same slice. Carbon has been plotted as a brown dotted line at 1/10 th of its original abundance. Scale bars: b, 10 nm; c, 5 nm.